The Korean Journal of Ceramics, **4** [3] 260 - 267 (1998)

Powder Preparation by Hydroxide Coprecipitation and Phase Development of $Pb_{0.97}La_{0.02}(Zr_{0.64}Sn_{0.25}Ti_{0.11})O_3$ Ceramics

Joon-Hyung Lee and Yet-Ming Chiang*

Department of Inorganic Materials Engineering
Kyungpook National University, Taegu 702-701, Korea
**Department of Materials Science and Engineering*
Massachusetts Institute of Technology, Cambridge 02139, U.S.A.
(Received July 26, 1998)

A homogeneous and stoichiometric fine powder of the ferroelectric $Pb_{0.97}La_{0.02}(Zr_{0.64}Sn_{0.25}Ti_{0.11})O_3$ (PLZST) has been prepared by the hydroxide coprecipitation method. Studies on the crystallization behavior of precursor as a function of temperature by X-ray powder diffraction and transmission electron microscopy techniques were consistent with the formation of the pyrochlore phase from amorphous, initially at low temperatures around 500~550°C. Further heat treatment up to 750°C resulted in development of the perovskite phase with no significant pyrochlore crystallite growth. At intermediate temperatures the precursor yields a fine mixture of pyrochlore and perovskite phases. When the pyrochlore phase was heat treated in air, slight weight increase was observed in the temperature range of 300~700°C, which is thought to be caused from oxygen absorption. In argon atmosphere, weight increase was not observed. On the other hand, weight loss began to occur near 700°C, with giving off mostly CO_2 gas. This implies that the pyrochlore phase seems to be crystallographycally and thermodynamically metastable. An apparent activation energy of 53.9 kcal/mol was estimated for the pyrochlore-perovskite phase transformation.

Key words : Ferroelectric, Coprecipitation, Pyrochlore, Perovskite, Phase

I. Introduction

Lead zirconate titanate stanate ceramics and further modified forms have been studied extensively for many potential applications in energy conversion such as actuator and shape memory.[1-4] These electrical and physical properties are directly related to the intrinsic crystal chemistry, composition, homogeneity and crystallization behavior of the materials.[5,6]

In Pb-based complex perovskite ceramics systems, PbO evaporates easily at higher temperature and forms undesirable phases.[7,8] The coexistence of an additional phase such as cubic pyrochlore phase deteriorates the ferroelectric properties and restricts many applications even if small amount of the phase exist.[9] Much effort has been expended to eliminate the cubic pyrochlore phase. Usually 5~15 mol% of excess PbO are added to compensate PbO loss during heating,[10,11] and columbite route which alters reaction sequence and leads to almost pyrochlore free phase is also employed.[12]

Generally, ceramic powders have been prepared by the solid-state reaction of the constituent metal oxides and carbonates. Such reactions often lead to compositional and structural inhomogeneities in the ceramics produced.[13,14] The powders prepared by non-oxide precursor routes are more homogeneous and reactive than those prepared by conventional solid-state reactions since the mixing of the reagents occurs on an atomic rather than a particulate scale.[15] In addition, the lower processing temperature can minimize the loss of PbO by evaporation and structural homogeneity will improve the ceramic physical properties. In these respect, the freeze drying method which converts the solution from a liquid to a solid state could be the most efficient method for maintaining chemical homogeneity and it also prevents segregation of components.

Recently, as the interests in ferroelectric films were renewed, extensive investigation has been accelerated and the development of metastable nonferroelectric pyrochlore and oxygen deficient pyrochlore phases of $A_2B_2O_7$ or $A_2B_2O_{7-\delta}$ at lower processing temperatures in Pb-containing ferroelectric thin films made by various methods was reported.[16-18] According to some literatures, the loss of lead due to its volatility during heating is the most important because local nonstoichiometry on the lead-poor side and may promote pyrochlore formation.[19] To compensate lead loss, it has become common practice to use precursors with some mol% of excess lead or, in the case of sputtering, to use targets containing up to 30% excess Pb(or PbO).[20] Other literature showed that the composition of pyrochlore is richer in Zr and more deficient in Pb than the perovskite phase.[21] The oxygen partial pressure dependence of the pyrochlore-perovskite phase formation was also reported.[22-24] On the other hand, a polycrystalline metastable Pb-Ti fluorite phase has been reported in the literature.[25] However the mechanism of the phase transformation is still unclear and the most of past studies have been reported in thin film process and there have been no systematic study of pyrochlore-perovskite

phase formation especially in ceramic powders.

In this study, ultra fine stoichiometric and homogeneous ferroelectric PLZST powder was prepared by coprecipitation method using freeze dryer. The pyrochlore phase development during heating and pyrochlore-perovskite phase transformation at higher temperature were analyzed using DTA-TG, ICP, gas mass spectrometer, X-ray, TEM, and HRTEM.

II. Experimental

$Pb(NO_3)_2$(99.9%), $La(NO_3)_36H_2O$(99.99%), $ZrOCl_38H_2O$ (99.9%), $SnCl_4$(99.99%), $TiCl_4$(99.999%) were used as starting chemicals. For preparing the titanium and tin source solutions, $TiCl_4$ and $SnCl_4$ were dissolved in 30% aqueous H_2O_2 in a glove box to prevent the hydrolytic precipitation of each hydroxide and the solutions were diluted to form a 0.1 mol dm^{-3} aqueous solution. $Pb(NO_3)_2$, $La(NO_3)_36H_2O$, $ZrOCl_28H_2O$ were dissolved in distilled water individually and diluted to a concentration of 0.1 mol dm^{-3}. The intrinsic acidity of mixed solution corresponding to the composition of $Pb_{0.97}La_{0.02}(Zr_{0.64}Sn_{0.25}Ti_{0.11})O_3$ was kept below pH=1 for perfect dissolving of precipitates. Since the PLZST ceramics are applicable for actuators by changing its volume during the phase transformation from antiferroelectric tetragonal (A_T) to ferroelectric rhombohedral (F_R) when electric field is applied,[26] the composition of $Pb_{0.97}La_{0.02}(Zr_{0.64}Sn_{0.25}Ti_{0.11})O_3$ on the phase boundary between A_T and F_R was selected as shown in Fig. 1. The PLZST solution was added in drops into a continuously stirring bath of NH_4OH solution whose pH was adjusted to 9. To compare the solubility behavior of individual metal hydroxides and to estimate the optimum coprecipitation condition, the solubility diagrams considered so far for individual hydroxides are superimposed in Fig. 2.

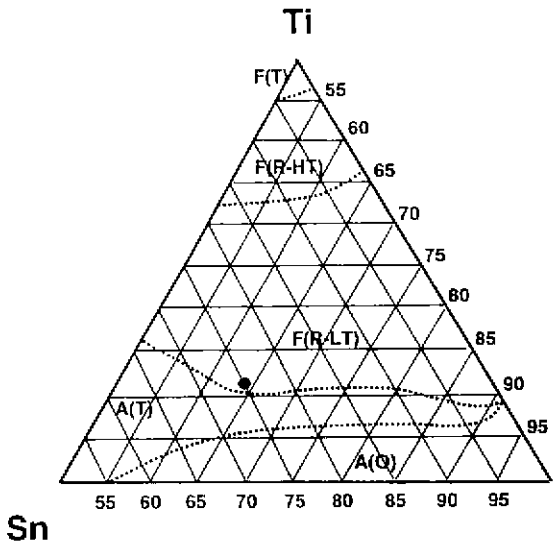

Fig. 1. Triaxial phase diagram for the system $Pb_{0.97}La_{0.02}$(Zr, Sn, Ti)O_3 at 25°C; specimens not poled.[26]

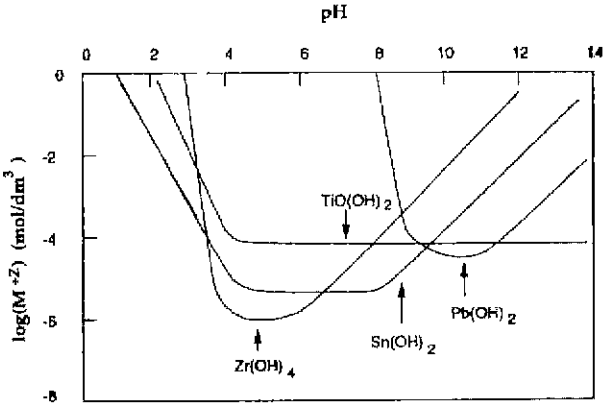

Fig. 2. Solubility diagram for the metal (Pb, Zr, Sn, Ti)-OH^- system.

It is apparent that a simultaneous precipitation region (triple point of solubility curves) of individual hydroxides cannot be found in the Pb-La-Zr-Sn-Ti system. In the pH range 5-6, Zr^{+4} and TiO^{+2} ions can be precipitated as hydroxides quantitatively, but Pb^{+2} ions will remain dissolved as soluble species such as $Pb_6(OH)_8^{+4}$ or will be precipitated as chlorides in chloride media. In the basic pH domain of pH=10-11, lead and titanium hydroxides can be formed quantitatively, while the $Zr(OH)_4$(s) will dissolve owing to the formation of soluble $Zr(OH)_5^-$ species. At pH 9 the lead and zirconium hydroxides will precipitate simultaneously along with the titanium hydroxide even though there are slight solubility differences between the hydroxides. Consequently, disregarding the formation of lead chlorides or lead carbonates, the optimum pH for the quantitative formation of a pure PLZST hydroxide precursor can be predicted by the solubility diagrams to be 9. Since the concentration of the corresponding metal solution was ca. 0.1 mol dm^{-3}, > 99% of metal hydroxide will precipitate at pH 9. During the coprecipitation, the pH of the bath was maintained at 9 with adding NH_4OH solution and the bath temperature was maintained at 60°C in order to dissolve any lead and tin chlorides formed during the mixing process.

After the precipitation the bath was cooled down to room temperature and held for 1 hour for equilibration. Then the precipitate was separated by decantation of supernatant liquid and washed several times with distilled water whose pH was adjusted to 9, to remove residual Cl^- and NO_3^- ions. The precipitate was sprayed into liquid nitrogen and freeze dried for maintaining chemical homogeneity and preventing powder agglomeration. The precipitate was calcined at various temperatures for 1 hour. ICP analysis was used for elemental analysis of the calcined powders and also for determining the residual metal ion concentration in the decanted solution after precipitation. Powder X-ray diffraction with nickel-filtered Cu-Kα radiation (Rigaku RTP 500 RC) was used for phase identification. For lattice parameter measurement, silicon standard powder (SRM 640B, NIST, U.

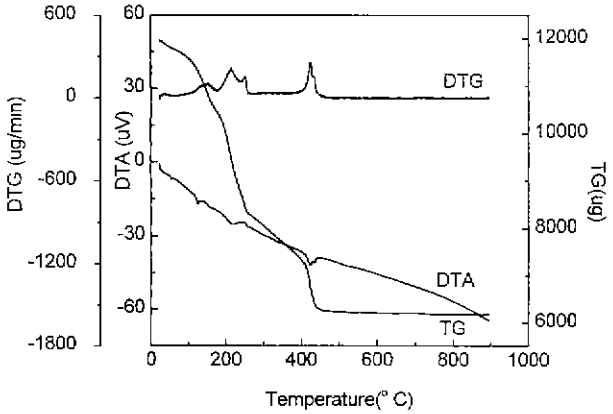

Fig. 3. Thermal analysis profile for the freeze dried precipitates. (air flowing rate 300 cc/min., heating ramp 5°C/min.)

S.A.) was added to the calcined powder. X-ray diffraction was performed with a step size of 0.002 degrees and a counting time per step of 1 second. High temperature X-ray (Rigaku RU 200) was used for kinetic analysis of pyrochlore-perovskite phase transformation with scanning the main peaks of 222 and 012 for pyrochlore and perovskite phase respectively. DTA-TG (Seiko, SSC/5200), gas mass spectrometer (Finnigan MAT 271), TEM (JEOL, JEM200CX) and HRTEM (ISI, EM002B) were also used for the characterization of powders.

III. Results and Discussion

Fig. 3 shows the DTA-TG-DTG curves for the freeze dried precipitates. The initial weight loss in the temperature range of 25~150°C was attributed to the liberation of surface-absorbed water and is accompanied by a weak endothermic DTA peak. The marked weight loss at 200~430°C in DTA and TG is due to the decomposition of hydroxy groups. The appearance of endothermic peaks at 450°C indicates the decomposition of metal-$(NO_3)_2$ into oxides as reported in a literature.[27] Therefore, a complete decomposition was expected to occurs around 450°C.

The ICP analysis was carried out for the powder calcined at 550°C, 1 h and the result is shown in Table 1. The final composition was shifted little bit to FR area.

Fig. 4 shows a series of X-ray diffraction patterns of the precipitates calcined for 1 hr at a series of increasing temperatures. After removal of hydroxy groups, solid-state reaction is believed to proceed. For a higher resolution of

Table. 1. ICP Result of Calcined Powder

Elements	Target Composition (mol)	Analyzed Value (mol)
Pb	0.970	0.983
La	0.020	0.006
Zr	0.640	0.631
Sn	0.250	0.251
Ti	0.110	0.128

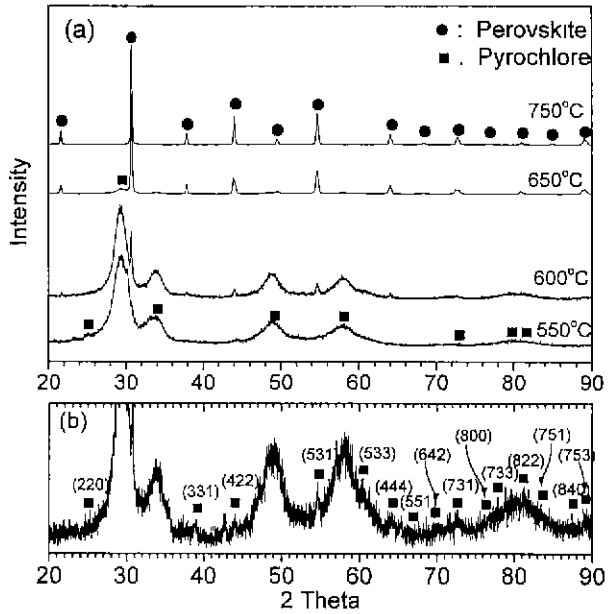

Fig. 4. (a) X-ray diffraction patterns of the precipitates calcined at a series of increasing temperature for a fixed calcining time of 1 h , and (b) magnified view of diffraction pattern calcined at 550°C.

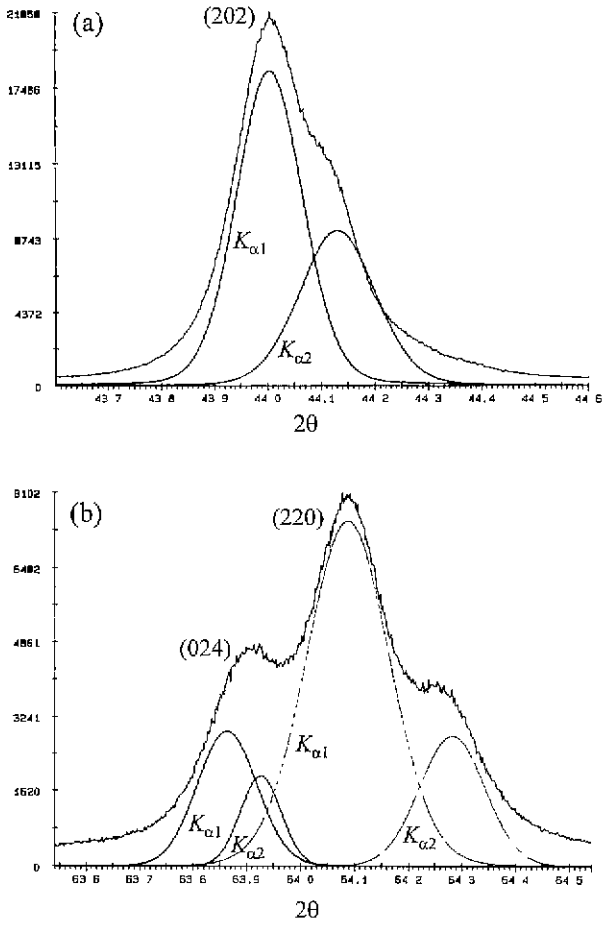

Fig. 5. Deconvoluted X-ray peaks of (a) (202) and (b) (024) and (220) corresponding to rhombohedral crystal structure.

X-ray diffraction, a step size of 0.002 degrees and a counting time per step of 1 sec were selected for the sample calcined at 550°C 1 h, and a magnified view of diffraction peaks are shown. Because of peak broadening and high background due to ultra fine particle size of powder, the superlattice reflections from pyrochlore phase were hardly identified. In this case, one can imagine a possibility of the existence of the fluorite structure, which has almost same diffraction patterns with the pyrochlore structure. Recently, Seifert et al.[25] reported a formation of the fluorite phase after pyrolysis of $PbTiO_3$ precursor on epitaxial growth by spin coating. However, in this experiment, the intensity of super lattice peaks from ultra fine pyrochlore phase($A_2B_2O_{7-\delta}$) are not strong enough though, they were clearly observed. The particle size of pyrochlore phase calculated by X-ray peaks was around 6 nm. With increasing temperature, perovskite PLZST phase started to appear. The single phase of the perovskite PLZST was obtained at 750°C. At intermediate temperatures between 550~750°C the precursor yields a mixture of pyrochlore and perovskite phases.

The deconvoluted X-ray peaks of 202, 024 and 220 with $K_{\alpha1}$ and $K_{\alpha2}$ corresponding to perovskite rhombohedral crystal structure are shown in Fig. 5. Calculated lattice parameters of rhombohedral perovskite and pyrochlore phase powders with silicon standard were 4.112Å, α= 89.838 and 10.005Å respectively.

Fig. 6 shows TEM micrographs of the pyrochlore-perovskite phase development in powders calcined at a) 450°C, b) 550°C and c) 650°C for 1 h. In Fig. 6 a), the powder has hollow like shape and its selected area electron diffraction (SAED) represents an amorphous like phase. In b), ultra fine but aggregation of powders into chain was shown. The crystallite size is on the order of 5~8 nm which is well matched with calculated

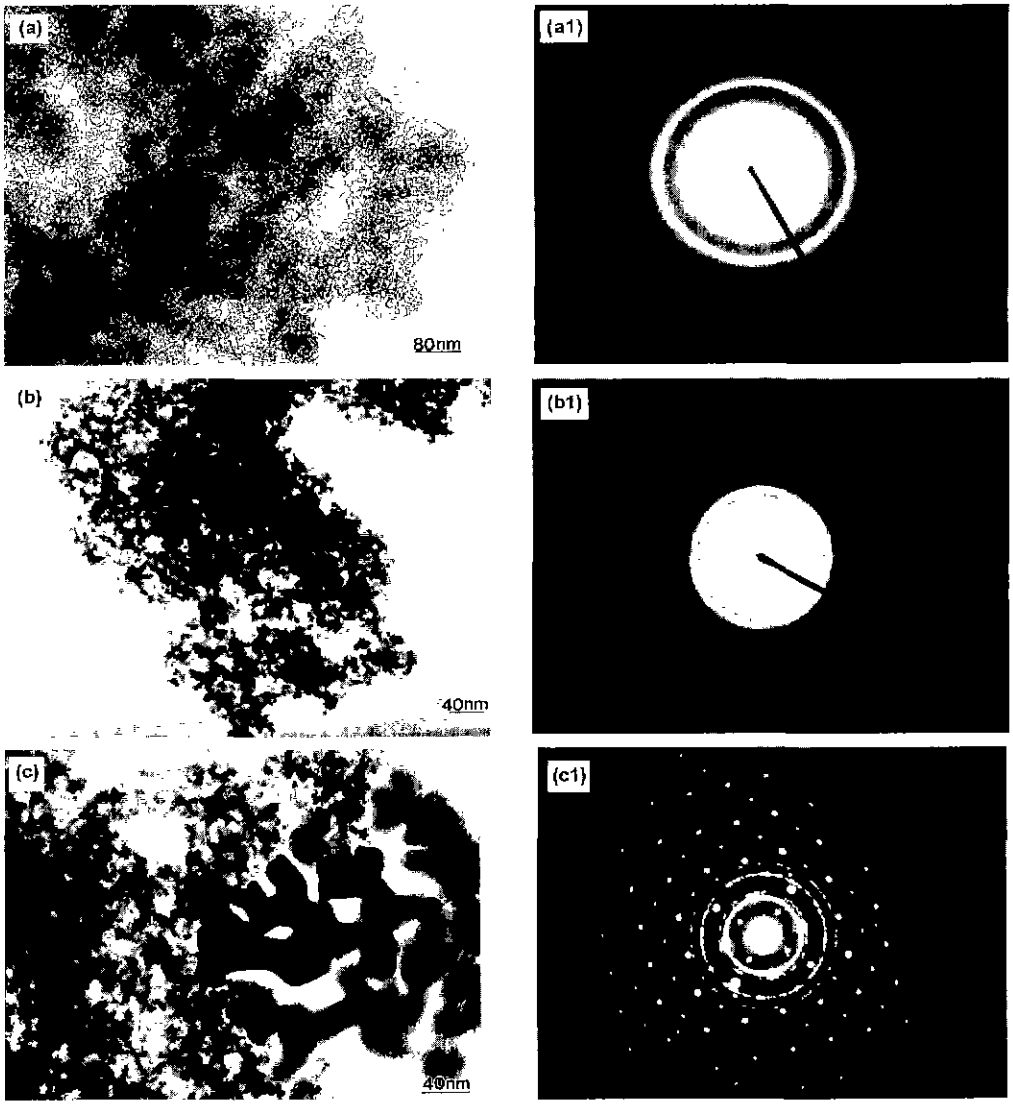

Fig. 6. TEM micrograph of pyrochlore-perovskite phase development of powders calcined at a) 450°C, b) 550°C and c) 650°C for 1 h, and its selected area electron diffraction (SAED) patterns.

Fig. 7. HRTEM image of powder calcined at 650°C for 1 hour.

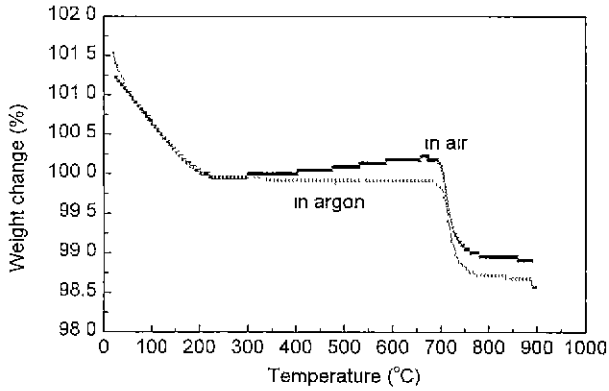

Fig. 8. TG analysis of pyrochlore phase powder in air and argon atmosphere. (air and argon flowing rate 300 cc/min., heating ramp 5°C/min.)

particle size by X-Ray diffraction. The SAED of nanocrystalline powder shows several diffused rings, which indicate very fine and relatively well-defined crystalline phase. d values as determined by SAED, were similar to reported d values for the principle reflections (i.e., 222, 400, 440, and 622) of a pyrochlore phase[28] with c=10.4Å. In the case of c), another crystallite phase with the order of 50~200 nm in particle size that forms a connected skeleton with each other was observed. This phase was identified to perovskite by powder X-ray diffraction and the SAED revealed a characteristic diffraction spot patterns of perovskite phase.

HRTEM was used to investigate the nucleation process and morphological features of nuclei for a sample that was calcined at 650°C for 1 hour. Fine but agglomerated pyrochlore with approximate 6 nm size and large perovskite phase are shown in Fig. 7. Both phases were well crystallized with different lattice fringe distances of 3.2 nm and 2.9 nm for pyrochlore and perovskite phase respectively. The composition analysis of the pyrochlore and perovskite phase was done using EDS attached STEM. However, any difference could not be found. A literature reported that a composition deviation between pyrochlore and perovskite is within $\pm 3\%$.[29] Considering the chemical homogeneity of the powder that was prepared by coprecipitation method, the composition of pyrochlore and perovskite appears to be the same except oxygen content, that is $A_2B_2O_6$ and $A_2B_2O_{7-\delta}$.

For a detail observation of thermogravimetric phenomena during heating (combustion) in air, DTA-TG was used in air and argon atmosphere for pyrochlore phase powder calcined at 550°C, 1 h, and the result is shown in Fig. 8. Weight loss from room temperature to 200°C is caused from evaporation of surface-absorbed water. When the sample was heat treated in air, approximately 0.3 % weight gain at 200~680°C and another weigh loss of 1.3% from 690 to 730°C were observed. In argon atmosphere, weight loss of 1.1% near 700°C appeared, but no weight gain from 200~680°C was observed. The final weak weight loss above 830°C in Fig. 8 may be due to the gradual evaporation of Pb. Assuming that pyrochlore PLZST phase has the ideal $A_2B_2O_7$ structure and changes to the perovskite structure of $A_2B_2O_6$, weight loss only by oxygen release is expected to be 2.27%/mol. Therefore, 0.3% of weight gain in oxygen atmosphere is thought to be caused from oxygen absorption to metastable $A_2B_2O_{7-\delta}$ pyrochlore phase in order to maintain local charge neutrality since the seventh oxygen ion is not needed for the stability of the octahedra frame work of pyrochlore structure of $Pb_2(Bx'B_{1-x}'')_2O_6\ O_{1-\delta}$ where $0 \leq \delta \geq 1$. The oxygen absorption will stabilize pyrochlore structure by decreasing δ value. After removing organic species such as OH^-, NO_3 etc, relatively long range diffusion is kinetically limited and thus pyrochlore could not have perfect crystalline structure from amorphous one. This metastable structure of pyrochlore becomes more stable as temperature goes up by diffusion of cations and anions. If the average charge on the B site differs from 4+, one can anticipate a corresponding change in the number of oxygen atoms occupying the seventh sites in order to maintain local charge balance. Local inhomogeneity may be able to change the average charge of B site additionally. During this process, oxygen might be absorbed or released due to unstable oxygen vacancy site of $A_2B_2O_{7-\delta}$. Cation and oxygen vacancy ordering have been observed in the crystallization of nonstoichiometric fluorites when exposed to higher heat-treatment temperatures.[25,30] From this result, it is believed that pyrochlore phase is thermodynamically stable at certain temperature range. This temperature range could be changed by various surrounding conditions such as oxygen partial pressure, homogeneity, etc.

The pyrolysis analysis using a gas mass spectrometer showed that the weight loss around 700°C was caused by mostly CO_2 gas release. Approximate calculation on this result implies that the 1/2 mol of pyrochlore phase contains C and O ions in the metastable structure and

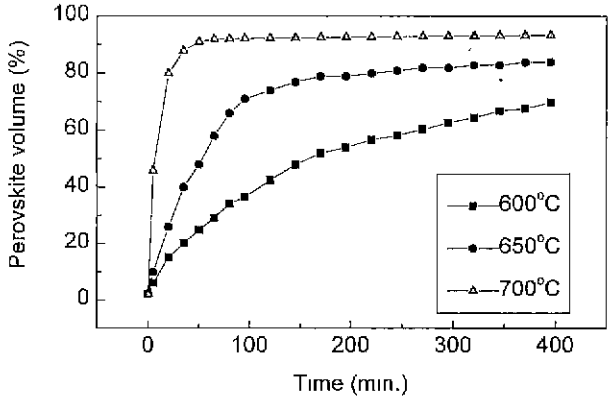

Fig. 9. Fractional perovskite PLZST as functions of time and temperature.

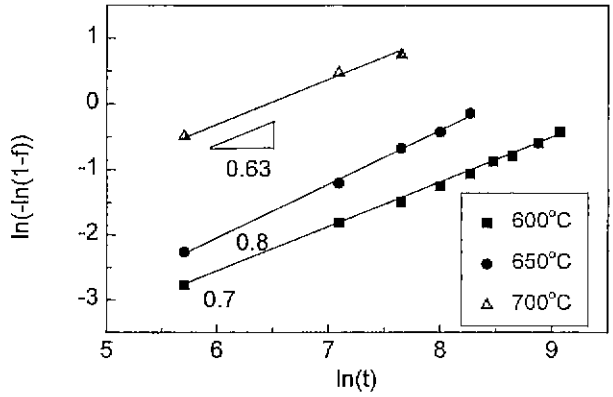

Fig. 10. Plot based on the Johson-Mehl-Avrami anayses of the kinetic data from Fig. 9.

the crystallization of the pyrochlore phase is an another example of kinetically limited crystallization.

Pyrochlore-perovskite transformation requires heating to temperature where long range diffusion becomes kinetically viable through reconstructing cation as well as anion sites from a simple cubic to a face-centered cubic arrangement. During this process, seventh oxygen in $A_2B_2O_{7-\delta}$ structure could be released and corresponding weight loss of $0 \leq \delta \leq 1$ is expected accompanying phase transformation from pyrochlore to perovskite. In argon atmosphere, we can not expect oxygen absorption thus weight gain was not shown in Fig. 8.

The reported results[22-24] of the effect of oxygen partial pressure on the perovskite phase formation, that is heat treatment or calcining in oxygen atmosphere hinder perovskite formation, is now understood by the viewpoint of oxygen release during phase transformation.

The kinetics of PLZST crystallization from pyrochlore phase is shown at three different temperatures in Fig. 9. In order to gain further insight into the factors controlling the hydrothermal formation of crystalline PLZST, a Johnson-Mehl-Avrami analysis was performed on the obtained kinetic data based on the following equation.[31,32]

$$\ln[-\ln(1-f)]=\ln(r)+m\ln(t)$$

where f is the fraction crystallized isothermally at time t, r is the rate constant that partially depends on nucleation frequency and growth rate and is very sensitive to temperature and m is the exponent constant that is independent of temperature but sensitive to the time dependence of the nucleation and growth rate and e geometry of particle. Hancock and Sharp[33] have shown that for reactions obeying a single theoretical rate expression, plots of -ln ln(1-f) against ln(t) over f=0.15-0.50 yield approximately straight lines with slopes m having a value falling within a range characteristic of three distinct reaction mechanisms. When m=0.54-0.62, a diffusion controlled mechanism is indicated, while a zero-order, first-order, or phase boundary controlled mechanism is indicated for m=1.0-1.24. A mechanism involving nucleation and growth control is indicated when m=2.0-3.0.

In Fig. 10, plots of -ln ln(1-f) against ln(t) over f=0.15-0.50 for the data in Fig. 9 are presented. Linear regression yields m value of 0.63-0.8. The result of 0.63 indicates a diffusion-controlled mechanism, and the other m values does not belong to any of the three mechanisms. However, it suggests a reaction mechanism described best in terms of diffusion controlled, which agreed with a literature of the bulk pyrochlore to perovskite phase transformation.[34]

An Arrhenius plot for the hydrothermal phase transformation from pyrochlore to perovskite is given in Fig. 11. The activation energy obtained in this way was 53.9 kcal/mol, which contains the activation energy of diffusion and the activation energy of nucleation also. This value is little bit smaller than those of reported activation energy of phase transformation in thin films from 59 up to 78 kcal/mol.[17,35,36] This difference may be caused by the composition difference between the systems.[37] As a result, it is believed that the processing methods does

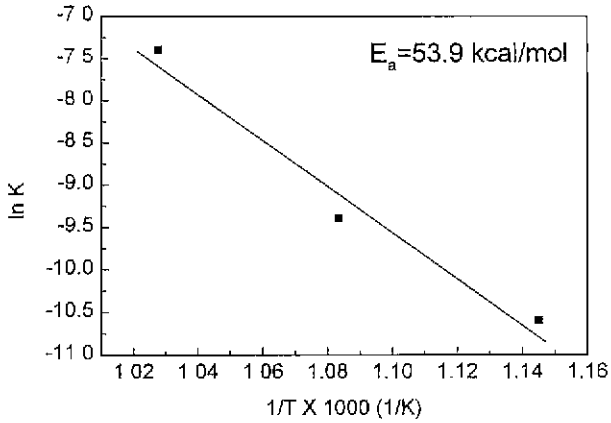

Fig. 11. Arrhenius plot for the hydrothermal phase transformation from pyrochlore to perovskite in PLZST. The activation energy is 53.9 kcal/mol.

not greatly affect on the activation energy of pyrochlore-perovskite phase transformation.

IV. Conclusions

Ultrafine PLZST powders were synthesized by coprecipitation method and the crystallization behavior was studied. At low temperatures around 500~550°C, pyrochlore phase was developed. Further heat treatment up to 750°C resulted in development of the perovskite phase with no significant pyrochlore crystallite growth. At intermediate temperatures the precursor yields a fine mixture of pyrochlore and perovskite phases.

The pyrolysis analysis using a gas mass spectrometer showed that weight loss is due to CO_2 gas release near 700°C, which implies that the pyrochlore phase seem to have the crystographycally and thermodynamically metastable structure. The activation energy obtained was 53.9 kcal/mol. Comparing to other reported activation energies, our processing method does not greatly affect on the activation energy of the pyrochlore-perovskite phase transformation.

Acknowledgment

This paper is a part of results of a project at M.I.T. during the stay for Post-Doc in 1995. Support from KOSEF is thankful.

References

1. W. Pan, Q. Zhang, A. Bhalla and L. E. Cross, "Field-Forced Antiferroelectric-to-Ferroelectric Switching in Modified Lead Zirconate Titanate Stanate Ceramics," *J. Am. Ceram. Soc.*, **72**(4), 571-578 (1989).
2. W Y. Pan, C. Q. Dam, Q. M. Zhang and L. E. Cross, "Large Displacement Transducers Based on Electric Field Forced Phase Transition in the Tetragonal $(Pb_{0.97}La_{0.02})$(Ti, Zr, Sn)O_3 Family of Ceramics," *J. Appl. Phys.*, **66**(12), 6014-6023 (1989).
3. K. G. Brook, J. Chen. K. R. Udayakumar and L. E. Cross, "Electric Field Forced Phase Switching in La-Modified Lead Zirconia Titanate Stanate Thin Films," *J. Appl. Phys.*, **75**(3), 1699-1704 (1994).
4. K. Ghandi and N. W. Hagood, "Shape Memory Ceramic Actuation of Adaptive Structures," Am. Ins. Of Aeronautics and Astronautics, AIAA-94-1758-CP, 221-231 (1994).
5. D. Viehland, D. Forst and J.-F. Li, "Compositional Heterogeneity and the Origins of the Multicell Cubic State in Sn-Doped Lead Zirconate Titanate Ceramics," *J. Appl. Phys.*, **75**(8), 4137-4143 (1994).
6. G. Arlt, D. Hennings and G. de With, "Dielectric Properties of Fine-Grained Bariun Titanate Ceramics," *J. Appl. Phys.*, **58**(4), 1619-1625 (1985).
7. R. L. Holman and R. M. Fulrath, "Intrinsic Nonstoichiometry in the Lead Zirconate-Lead Titanate System Determined by Knudsen Effusion," *J. Appl. Phys.*, **44**(12), 5227-5236 (1973).
8. T. Tani and D. A. Payne, "Lead Oxide Coatings on Sol-Gel-Derived Lead Lanthanum Zirconate Titanate Thin Layers for Enhanced Crystallization into the Perovskite Structure," *J. Am. Ceram. Soc.*, **77**(5), 1242-1248 (1994).
9. B. Tuttle, R. W. Schwartz, D. H. Doughty and I. A. Voigt, "Characterization of Chemically Prepared PZT Thin Films"; pp.159-65 in *Ferroelectric Thin Films*, Proceedings of the Materials Research Society Symposium (San Francisco, CA. April, 1990). Edited by E. R. Myers and A. I, Kingon, Materials Research Society, Pittsburgh, PA, 1990.
10. B. A. Tuttle, J. A. Voigt, D. C. Goodnow, D. L. Lamppa, T. J. Headley, M. O. Eatough, G. Zeuder, R. D. Nasby, and S. M. Rodgers, "Highly Oriented, Chemically Prepared Pb)Zr,Ti)O_3 Thin Films," *J. Am. Ceram. Soc.*, **76**(6), 1537-1544 (1993).
11. J. F. Chang and S. B. Desu, "Effects of Dopants in PZT films," *J. Mater. Res.*, **9**(4), 955-969 (1994).
12. S. L. Swartz and T. R. Shrout, "Fabrication of Perovskite Lead Magnesium Niobate," *Mat. Res. Bull.*, **17**, 1245-1250 (1982).
13. J. Thomson, Jr, "Chemical Preparation of PLZT Powders from Aqueous Nitrate Solutions," *Am. Ceram. Soc. Bull.*, **53**(5), 421-433 (1974).
14. C. D. Chandler, C. Roger and M. J. Hampden-Smith, "Chemical Aspects of Solution Routes to Perovskite-Phase Mixed-Metal Oxides from Metal-Organic Precursors," *Chem. Rev.*, **93**, 1205-1241 (1993).
15. R. Roy, "Ceramics by the Solution-Sol-Gel Route," Science, **238**, 1664-1669 (1987).
16. S. A. Mansour, G. L. Liedl, and R. W. Vest, "Microstructural Developments and Dielectric Properties of Rapid Thermally Processed PZT Thin Films Derived by Metallo-organic Decomposition," *J. Am. Ceram. Soc.*, **78**(6), 1617-1623 (1995).
17. C. K. Kwok and S. B. Desu, "Pyrochlore-Perovskite Phase Transformation of Lead Zirconate Titanate (PLT) Thin Films"; pp. 85-97 in Ceramic Transactions Vol. 25: Ferroelectric Films Edited by A. S. Bhalla and K. M. Nair, American Ceramic Society, Westerville, 1992.
18. C. H. Peng and S. B. Desu, "Structure Development Study of Pb(Zr,Ti)O_3 Thin Films by an Optical Method," *J. Am. Ceram. Soc.*, **77**(6), 1486-1492 (1994).
19. M. Ishida, H. Matsunami and T. Tanaka, "Preparation and Properties of Ferroelectric PLZT Thin Films by RF Sputtering," *J. Appl. Phys.*, **48**(3), 951-953 (1997).
20 K. Iijima, R. Takayama, Y. Tomita and I Ueda, "Epitaxial Growth and the Crystallographic, Dielectric, and Pyroelectric Properties of Lanthanum-Modified Lead Titanate Thin Films," *J. Appl. Phys.*, **60**(8), 2914-2919 (1986).
21. A. H. Carim, B. A. Tuttle, D. H. Doughty and S. L. Martinez, "Microstructure of Solution-Processed Lead Zirconate Titanate (PZT) Thin Films," *J. Am. Ceram. Soc.*, **74**(6), 1455-1458 (1991).
22. L. A. Bursill and K. G. Brooks, "Crystallization of Sol-Gel Derived Lead-Zirconate-Titanate Thin Films in Argon and Oxygen Atmospheres," *J. Appl. Phys.*, **75**(9), 4501-4509 (1994).
23. G. R. Fox and S. B. Krupanidhi, "Dependence of

Perovskite/Pyrochlore Phase Formation on Oxygen Stoichiometry in PLT Thin Films," *J. Mater. Res.*, **9**(3), 699-711 (1994).

24. K. G. Brooks, I. M. Reaney, R. Klissurska, Y. Huang, L. Bursill, and N. Setter, "Orientation of Rapid Thermally Annealed Lead Zirconate Titanate Thin Films on (111) Pt Substrates," *J. Mater. Res*, **9**(10), 2540-2553 (1994).
25. A. Siefert, F. F. Lange, and J. S. Speck, "Epitaxial Growth of $PbTiO_3$ Thin Films on (001) $SrTiO_3$ From Solution Precursors," *J. Mater. Sci.*, **10**(3), 680-691 (1995).
26. D. Berlincourt, "Transducers Using Forced Transitions Between Ferroelectric and Antiferroelectric States," IEEE Transactions on Sonics and Ultrasonics, **13**(4), 116-125 (1966).
27. K. L. Yadav and R. N. P. Choudhary, "Synthesis and Characterization of PLZT (10/65/35)," *J. Mater. Sci.*, **28**, 765-772 (1993).
28. C. K. Kwok and S. B. Desu, "Pyrochlore to Perovskite Phase Transformation in Sol-Gel Derived Lead-Zirconate-Titanate Thin Films," *Appl. Phys. Lett.*, **60**(12), 1430-1432 (1992).
29. Z. Surovyak, A. A. Bakirov, I. N. Zakharchenko, E. V. Sviridov, V. A. Aleshin, and A. E. Panich, "Thin Films of $Pb_2(Zr_{1-x}Ti_x)_2O_6$ with the Pyrochlore Structure," *Inorganic Materials*, **31**(8), 1004-1006 (1995).
30. V. Jayaram, M. DeGraef and C. G. Levi, "Metastable Extension of the Fluorite Phase Field in Y_2O_3-ZrO_2 and its Effect on Grain Growth," *Acta Metall. Mater.*, **42**(6), 1829-1846 (1994).
31. M. Avrami, "Kinetincs of Phase Change I: General Theory," *J. Chem. Phys.*, **7**(12), 1103-1112 (1939).
32. M. Avrami, "Granulation, Phase Change, and Microstructure: Kinetincs of Phase Change III," *J. Chem. Phys.*, **9**(2), 177-184 (1941).
33. J. D. Hancock and J. H. Sharp, "Method of Comparing Solid-State Kinetic Data and Its Application to the Decomposition of Kaolinite, Brucite, and $BaCO_3$," *J Am. Ceram. Soc.*, **55**(2), 74-77 (1972).
34. H. M. Jang, S. R. Cho and K. M. Lee, "Mechanism of Formation of Perovskite Phase and Dielectric Properties of $Pb(Zn,Mg)_{1/3}Nb_{2/3}O_3$ Ceramics Prepared by Columbite Precursor Routes," *J. Am. Ceram. Soc.*, **78**(2), 297-304 (1995).
35. E. M. Griswold, L. Weaver, I. D. Calder and M. Sayer, "Rapid Thermal Processing and Crystallization Kinetics in Lead Zirconate Titanate (PZT) Thin Films," *Mat. Res Soc. Symp. Proc.*, **361**, 389-394 (1995).
36. Y. Yoshikawa and K. Tsuzuki, "Crystallization of Fine, Chemically Prepared Lead Lanthanum Zirconate Titanate Powders at Low Temperatures," *J. Am. Ceram. Soc.*, **73**(1), 31-34 (1990).
37. S. Y. Chen, C. M. Wang and S. Y. Cheng, "Reaction Kinetics of Perovskite Phase Formation in Lead Zinc Magnesium Niobate Ceramics." *J. Am. Ceram. Soc.*, **74**(10), 2506-2512 (1991).